European Heart Journal (2013) **34**, 1134–1146
doi:10.1093/eurheartj/ehs349

FASTTRACK BASIC SCIENCE

Murine and human pluripotent stem cell-derived cardiac bodies form contractile myocardial tissue *in vitro*

George Kensah[1†], Angelica Roa Lara[1†], Julia Dahlmann[1], Robert Zweigerdt[1], Kristin Schwanke[1], Jan Hegermann[2], David Skvorc[1], Anke Gawol[1], Azadeh Azizian[3], Stefan Wagner[3], Lars S. Maier[3], Andreas Krause[4], Gerald Dräger[4], Matthias Ochs[2], Axel Haverich[1], Ina Gruh[1‡], and Ulrich Martin[1*‡]

[1]Leibniz Research Laboratories for Biotechnology and Artificial Organs, Department of Cardiac, Thoracic, Transplantation and Vascular Surgery, Hannover Medical School, Cluster of Excellence REBIRTH, Carl-Neuberg-Str. 1, 30625 Hannover, Germany; [2]Institute of Functional and Applied Anatomy, Hannover Medical School, Hannover, Germany; [3]Department of Cardiology and Pneumology, Georg-August-Universitaet Goettingen, Goettingen, Germany; and [4]Institute of Organic Chemistry, Center of Biomolecular Drug Research (BMWZ), Leibniz University Hannover, Hannover, Germany

Received 26 June 2012; revised 7 September 2012; accepted 27 September 2012; online publish-ahead-of-print 26 October 2012

Aims We explored the use of highly purified murine and human pluripotent stem cell (PSC)-derived cardiomyocytes (CMs) to generate functional bioartificial cardiac tissue (BCT) and investigated the role of fibroblasts, ascorbic acid (AA), and mechanical stimuli on tissue formation, maturation, and functionality.

Methods and results Murine and human embryonic/induced PSC-derived CMs were genetically enriched to generate three-dimensional CM aggregates, termed cardiac bodies (CBs). Addressing the critical limitation of major CM loss after single-cell dissociation, non-dissociated CBs were used for BCT generation, which resulted in a structurally and functionally homogenous syncytium. Continuous *in situ* characterization of BCTs, for 21 days, revealed that three critical factors cooperatively improve BCT formation and function: both (i) addition of fibroblasts and (ii) ascorbic acid supplementation support extracellular matrix remodelling and CB fusion, and (iii) increasing static stretch supports sarcomere alignment and CM coupling. All factors together considerably enhanced the contractility of murine and human BCTs, leading to a so far unparalleled active tension of 4.4 mN/mm^2 in human BCTs using optimized conditions. Finally, advanced protocols were implemented for the generation of human PSC-derived cardiac tissue using a defined animal-free matrix composition.

Conclusion BCT with contractile forces comparable with native myocardium can be generated from enriched, PSC-derived CMs, based on a novel concept of tissue formation from non-dissociated cardiac cell aggregates. In combination with the successful generation of tissue using a defined animal-free matrix, this represents a major step towards clinical applicability of stem cell-based heart tissue for myocardial repair.

Keywords Embryonic stem cells • Induced pluripotent stem cells • Cardiac differentiation • Myocardial tissue engineering

Introduction

Current therapeutic strategies targeting cardiovascular diseases include the enhancement of endogenous regeneration,[1,2] the injection of single cells,[3–5] or the application of bioartificial tissue constructs.[6–8]

The identification of a suitable cell source is one of the most critical aspects of myocardial tissue engineering. Pluripotent stem cells (PSCs), i.e. embryonic stem cells (ESCs),[9,10] and induced PSCs (iPSCs)[11,12] hold the capability of differentiating into cells of all three germ layers, including cardiomyocytes (CMs).[13–16] Recent advance in reprogramming technology including generation of transgene-free iPSCs,[17] raised expectations on the clinical application of iPSCs in the foreseeable future. Engraftment and long-term survival of iPSC-derived CMs (iPSC–CMs) has been

† These authors contributed equally as first authors. ‡These authors contributed equally as senior authors.

* Corresponding author. Tel: +49-511-532-8820/8821, Fax: +49-511-532-8819, Email: martin.ulrich@mh-hannover.de

demonstrated in small animal hearts already.[18–20] However, large areas of structurally integrated *de novo* myocardium have not been observed. Moreover, despite demonstration of electric coupling, the recently observed functional improvements were typically rather modest and far from restoring healthy heart function *in vivo*.[4,21,22] To date, the underlying reasons are not entirely clear. Much likely, the way of surgical delivery is one major limitation and the transplantation of contractile myocardial patches might be beneficial in terms of long-term cell retention, survival, and function. Moreover, and in contrast to cellular therapies, engineered myocardial tissue might enable replacement of scar tissue after infarction and reconstruction of congenital malformations. In animal models, functional tissue generated *in vitro* from primary cells was demonstrated to support the failing heart.[6,7]

So far, PSC-based engineered myocardial-like tissue has been generated almost exclusively using ESC derivatives after cardiac differentiation in embryoid bodies (EBs), which contain non-cardiac cell types as well,[23] including persisting PSCs.[18] However, for well-structured heart tissue without interfering extra-myocardial components, and to avoid teratoma formation after transplantation,[24] rigorous purification of CMs, and removal of residual PSCs will be mandatory. Some studies used murine ESC-derived CMs (ESC-CMs) enriched by Percoll gradient centrifugation to generate contractile cardiac tissue.[25,26] Cardiomyocytes purified from transgenic cell lines expressing antibiotic resistance genes under control of the cardiac α-myosin heavy-chain (α-MHC, MYH6) promoter were combined with collagen- or fibrin-based matrices,[27–29] or with the thermo-responsive cell sheet technology.[30] Recently, Tulloch *et al.*[31] provided proof-of-concept that tissue engineering protocols for human ESC–CMs can also be applied to human iPSC–CMs.

Despite recent progress, current stem cell-based engineered cardiac tissue is certainly not comparable with native heart tissue, and few studies, only, have reported measurable contraction forces of engineered cardiac tissue derived from murine[25,29] or human stem cells,[23,31] all using undefined animal-derived matrix components, such as Matrigel™ or Geltrex™.

In this study, to the best of our knowledge, it is the first time that the potential of highly purified CMs derived from murine iPSCs, human ESCs as well as human iPSCs, to produce functional bioartificial cardiac tissue (BCT) is demonstrated. Our study combined for the first time a new stimulation strategy for tissue maturation with a novel concept of tissue formation from non-dissociated cardiac bodies (CBs), together leading to a dramatic increase in contractile forces, now comparable with native myocardium. In addition, we implemented a defined animal-free matrix based on pure human collagen and hyaluronic acid for human stem cell-based engineered heart tissue, all together representing a major step towards clinical applicability for myocardial repair.

Methods

Generation and selection of cardiomyocytes from murine induced pluripotent stem cells

Murine iPSCs were genetically modified to express a Zeocin™ resistance gene under control of the cardiac-specific α-MHC (MYH6) promoter (see Supplementary material online, *Figure S1*). Cardiac differentiation was initiated by EB formation in hanging drops. Antibiotic-mediated selection of CMs from transgenic murine iPSCs was initiated on differentiation day (dd) 7 by medium supplementation with 400 μg/mL Zeocin™ (Life Technologies, Darmstadt, Germany), leading to CM-enriched aggregates termed CBs, which were characterized by immuno-staining, quantitative real-time polymerase chain reaction (PCR), patch clamp analysis, and microelectrode arrays (MEAs) (see Supplementary material online, *Figure S2*).

Generation and selection of cardiomyocytes from human embryonic stem cells and human induced pluripotent stem cells

Human ESCs and human iPSCs were modified to express a neomycin-resistance gene under control of the MYH6 promoter (see Supplementary material online, *Figure S6A and B*). For human ESCs, cardiac differentiation was initiated by spontaneous EB formation in suspension culture.[24] For human iPSCs, EB formation was induced in V-bottom 96-well plates.[32] Antibiotic-mediated selection of CMs was started 3 days after first contractions were observed using 200 μg/mL G418 (Sigma-Aldrich, Steinheim, Germany) to generate human PSC-derived CBs (see Supplementary material online, *Figure S6C–G*).

Bioartificial cardiac tissue preparation and cultivation

As described previously, BCT was prepared from a mixture of liquid collagen type I and Matrigel™[33,34] (or hyaluronic acid) (Dahlmann *et al.*, in press)[35] combined with cells in a volume of 220 μL (see Supplementary material online, *Figure S3A*). Two strategies for the preparation of murine BCTs were compared: (i) use of dissociated iPSC-derived CMs and (ii) direct use of selected CBs for tissue preparation on dd14, both with different amounts of γ-irradiated murine fetal fibroblasts. Non-selected EBs were used as controls. For human BCTs, non-dissociated G418-selected human CBs were used with γ-irradiated human foreskin fibroblasts. Tissue constructs were subject to constant static stress due to fixation at both ends, at a length of 6 mm. Additional mechanical stretch was applied in a custom-made bioreactor,[34] using either uniaxial cyclic stretch or stepwise growing static stretch (see Supplementary material online, *Figure S3B* and *C*). Tissue formation was monitored microscopically; vital CMs were visualized based on their high metabolic activity with 50 nM tetramethylrhodamine methyl ester (TMRM), selectively staining mitochondria-rich cells.[36] Direct measurements of active contraction and passive force were performed using the bioreactor force sensors.[34]

Gene expression analysis and assessment of tissue morphology

Gene expression of cells and BCTs was analysed using semi-quantitative RT–PCR or quantitative real-time PCR after RNA isolation and reverse transcription. Immuno-fluorescence staining was used to assess protein expression and to analyse the sarcomere length of CMs within BCTs. Tissue structure and (sub-)cellular organization was analysed by transmission electron microscopy.

Statistical analysis

Statistical analysis was performed with GraphPad Prism software (version 5.03 for Windows; GraphPad Software). Values reported are means and standard errors of the mean. Unless stated otherwise, data were analysed by two-way analysis of variance (ANOVA), with the Bonferroni *post hoc* test for comparison of any two groups; one-way ANOVA was used for analysis of unrelated groups as shown in *Figures 3C–H*, *5*, and *7F* and *G*. $P \leq 0.05$ were considered significant.

Results

Efficient genetic selection of differentiated murine induced pluripotent stem cell derivatives generates cardiac bodies composed of functional cardiomyocytes

Murine iPSCs were genetically modified for antibiotic selection of CMs based on integration of a Zeocin^{TM}-resistance gene under control of the cardiac α-MHC (MYH6) promoter (see Supplementary material online, *Figure S1A* and *B*). Zeocin^{TM} was found to efficiently enrich CMs within differentiated EBs, resulting in TMRM^{bright} contracting CBs within 7 days of selection (see Supplementary material online, *Figure S1C–F*). Selected CBs represent a three-dimensional culture of almost pure CMs (>99% cTnT^{+} cells, see Supplementary material online, *Figure S1I* and *K*), and their functionality was demonstrated by immuno-staining, quantitative real-time PCR, patch clamp analysis, and microelectrode arrays (MEA) (see Supplementary material online, *Figure S2*). Action potential analysis detected mostly ventricle- and pacemaker-like cells (both 41%) and fewer atrial-like and Purkinje-like CMs (both 9%) (see Supplementary material online, *Figure S2* and *Table S3*). Non-genetic selection of murine iPSC–CMs by fluorescence activated cell sorting (FACS) of TMRM^{bright} cells was also feasible, yet by far less efficient: Zeocin^{TM} selection of transgenic murine iPSCs resulted in >100-fold higher cell yields of 1.6 ± 0.3 viable cells/iPSC (initially inoculated for differentiation) than TMRM-based sorting (0.013 ± 0.005 cell per iPSC) (see Supplementary material online, *Figure S1G–L*). Consequently, to obtain sufficient cell numbers for cardiac tissue engineering, we used the antibiotic selection approach for all following experiments.

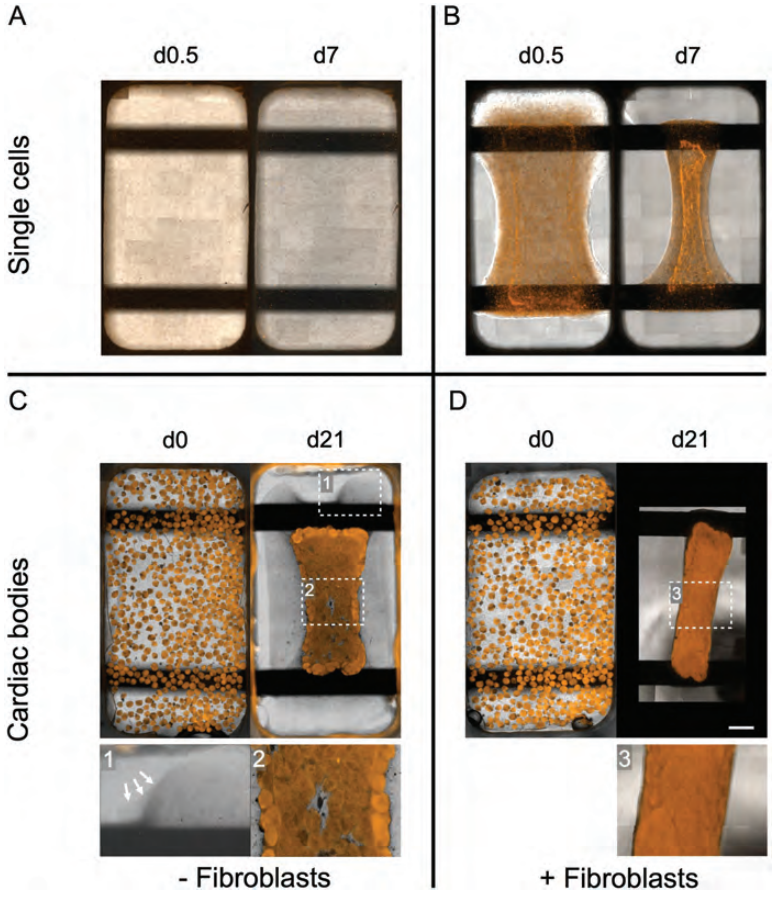

Figure 1 Fibroblasts are essential for bioartificial cardiac tissue formation from murine induced pluripotent stem cell-derived dissociated cardiomyocytes and whole cardiac bodies. (*A*) Bioartificial cardiac tissue containing single cell dissociated cardiomyocytes, only, did not consolidate and tetramethylrhodamine methyl ester fluorescence as indicator of cardiomyocyte viability decreased. (*B*) Addition of fibroblasts led to rapid remodelling of the matrix and improved cardiomyocyte survival. (*C*) α-Myosin heavy-chain Zeo^{R} selected cardiac bodies without fibroblasts resulted in bioartificial cardiac tissue with incomplete extracellular matrix remodelling (see arrows in magnified image 1), incomplete cardiac body fusion (see magnified image 2) and lack of stability. (*D*) α-Myosin heavy-chain Zeo^{R} selected cardiac bodies with 10% fibroblasts led to efficient cardiac body fusion (see magnified image 3), with long-term survival of actively contracting bioartificial cardiac tissue without re-emergence of Oct3/4-eGFP^{+} cells. Scale bar: 1 mm. See also Supplementary material online, *Figures S1 and S2* and *Movie S1*.

Generation of functionally and structurally homogenous myocardial tissue from murine induced pluripotent stem cell-derived cardiac bodies is fibroblast dependent

Previous reports demonstrated the importance of fibroblasts for CM survival, coupling, and generation of functional and well-structured myocardial tissue.[7,28,29] Therefore, murine iPSC–CMs, enzymatically dissociated into single cells from Zeocin™-selected CBs, were mixed with different amounts (0–25%) of mitotically inactivated murine foetal (embryonic day 13) fibroblasts and a Matrigel™/collagen I-based matrix (see Supplementary material online, *Figure S3*). As expected from the literature, addition of fibroblasts was essential for solid tissue formation, and increased CM metabolism and viability (*Figure 1A* and *B*). However, even with the optimal amount of fibroblasts, the use of single-cell murine iPSC–CMs sparsely resulted in spontaneously and

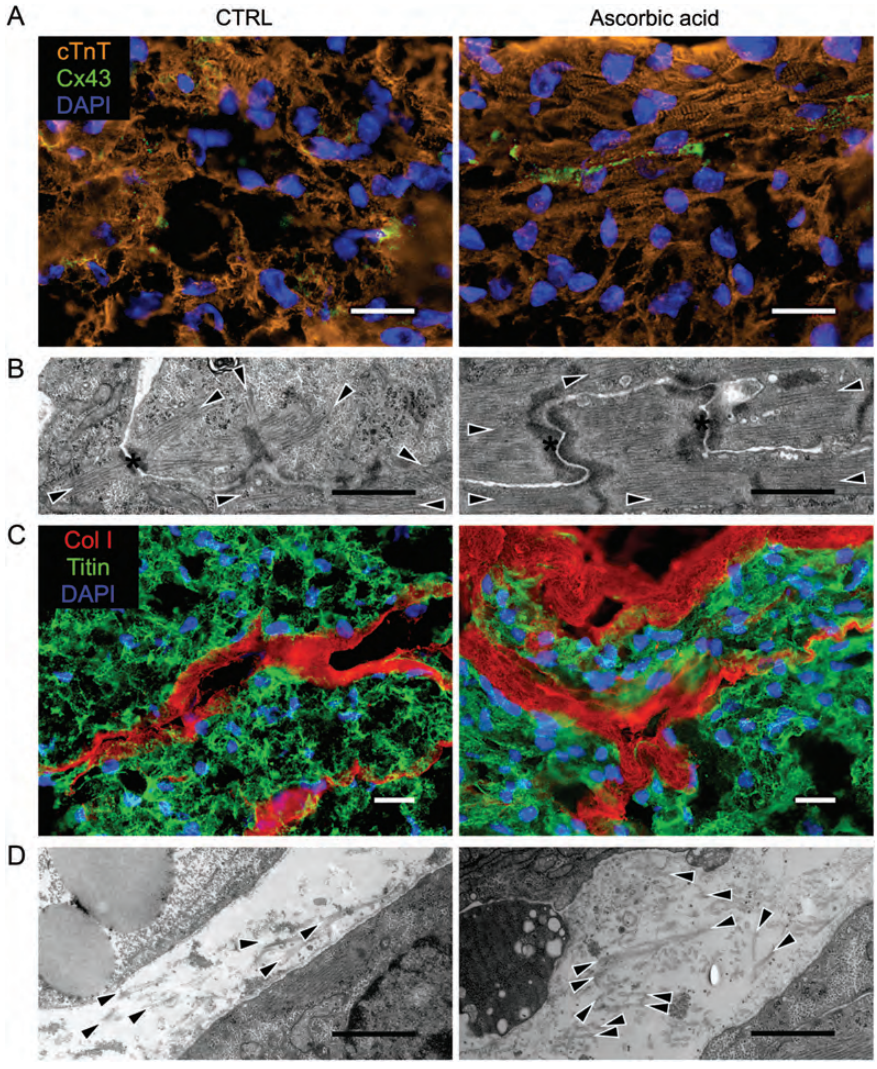

Figure 2 Ascorbic acid critically affects murine induced pluripotent stem cell-derived bioartificial cardiac tissue morphology and extracellular matrix organization. (*A*) Immuno-fluorescence staining against cTnT (red)/connexin 43 (green) in sections of cardiac body/fibroblast-based induced pluripotent stem cell-derived bioartificial cardiac tissue cultivated under control conditions (left) or with ascorbic acid (right); ascorbic acid-treated bioartificial cardiac tissue showed areas with longitudinally arranged (anisotropic) cardiomyocytes with distinct cross-striation (see upper part). (*B*) Transmission electron microscopy showed more prominent cell–cell contacts between cardiomyocytes (intercalated discs, asterisks) in ascorbic acid-treated bioartificial cardiac tissue and improved orientation of sarcomeres (arrowheads). (*C*) Immuno-fluorescence staining against collagen type I (red)/titin (green) showed more prominent collagen fibre bundles in the ascorbic acid-treated group. (*D*) Transmission electron microscopy showed accumulation of collagen in the intracellular space next to cardiomyocytes and more collagen fibrils (arrowheads) in ascorbic acid-treated bioartificial cardiac tissue. (A) and (C): nuclei stained with DAPI (blue); scale bars: 20 μm. (B) and (D): scale bars: 1 μm.

simultaneously contracting tissue constructs, with maximum active forces between 150 and 500 μN ($n = 30$; data not shown).

In a novel straightforward approach, we directly used whole CBs for the preparation of BCT to prevent disruption of pre-formed functional cell–cell contacts and major CM death. Cardiac bodies without fibroblast supplementation resulted in the formation of contractile BCTs with CBs fused to some extent, however, with incomplete extracellular matrix (ECM) remodelling and consolidation (*Figure 1C* and see Supplementary material online, *Movie S1*) as well as lack of stability, preventing force measurements. We found that a fibroblast content between 8 and 17% resulted in efficient fusion of CBs over time (see Supplementary material online, *Movie S1*) and formation of spontaneously and simultaneously contracting well-organized tissue with high density of viable $TMRM^{bright}$ CMs after 21 days of cultivation (*Figure 1D*). A fibroblast content of 10% generated BCTs with the highest active forces of 0.75 ± 0.06 mN measured on d21 (see Supplementary material online, *Figure S3E*) and therefore was used for all further experiments. In contrast, the use of non-selected EBs together with fibroblasts resulted in the formation of disorganized tissue with persistent pluripotent cells, large cystic outgrowths, and impaired contractility (see Supplementary material online, *Figure S3F*).

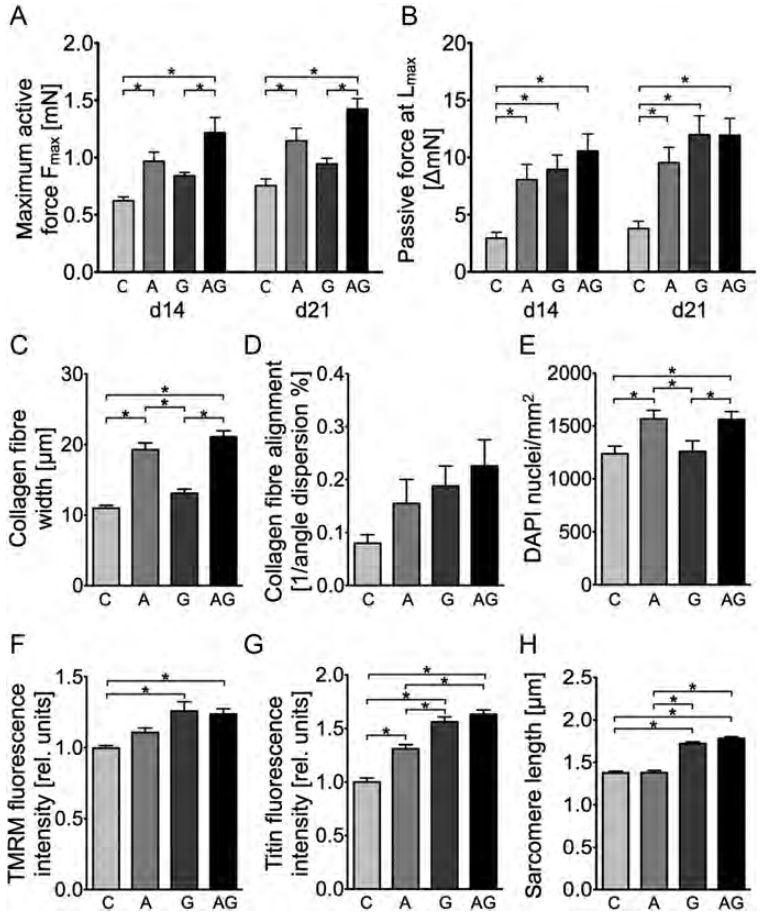

Figure 3 Comprehensive overview on functional and structural parameters of murine induced pluripotent stem cell-derived bioartificial cardiac tissue. (*A*) Maximum forces of murine induced pluripotent stem cell-derived bioartificial cardiac tissue from different treatment groups: C, control; A, ascorbic acid; G, G-stretch; AG, ascorbic acid and G-stretch; maximum contraction forces (F_{max}) measured after electrical pacing (25 V, 5 ms) showed high impact of AA and moderate influence of G-stretch on d14 and d21. (*B*) Passive forces increased over time (d14 to d21) and were significantly higher after ascorbic acid-treatment and G-stretch. (*C*) Analysis of bioartificial cardiac tissue sections immuno-stained against collagen type I showed strong influence of ascorbic acid on fibre width and alignment (in *D*, given as [1/angle dispersion %]), and of G-stretch on alignment only. (*E*) Numbers of DAPI-stained nuclei per mm^2 were significantly increased for ascorbic acid-treated bioartificial cardiac tissue. (*F*) Fluorescence intensities of TMRM in viable bioartificial cardiac tissue were moderately increased with ascorbic acid and significantly with G-stretch. (*G*) Both ascorbic acid and G-stretch significantly increased fluorescence intensities of titin staining of fixed cryosections. (*H*) Sarcomere length, determined in cross-striated cardiomyocytes after cardiac troponin T staining, was significantly increased in G-stretched bioartificial cardiac tissue. All columns are means ± SEM, $n = 8–9$ for (A) and (B), $n = 83–112$ for (C), $n = 75–90$ for (D), $n = 15–20$ areas (0.3 mm^2) for (E), (F) and (G), $n = 77–184$ for (H). $^*P \leq 0.05$; one-way analysis of variance for (C)–(H). See also Supplementary material online, *Figure S3* and *Movie S2*.

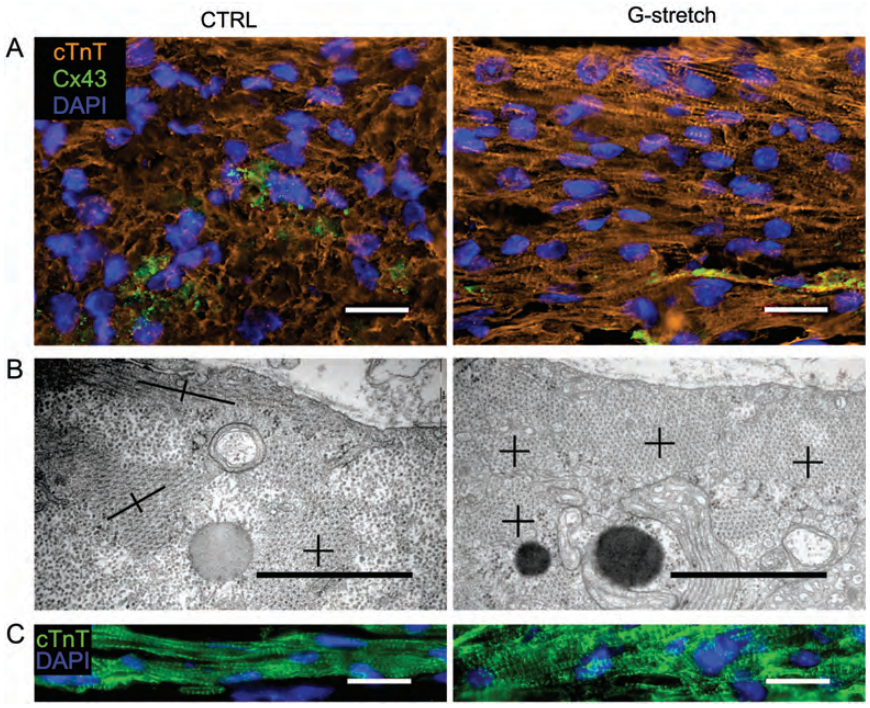

Figure 4 Growing stretch improves structure and sub-cellular organization of murine induced pluripotent stem cell-derived bioartificial cardiac tissue. (*A*) Immuno-fluorescence staining against cTnT (red)/connexin 43 (green) of cardiac body/fibroblast-based murine induced pluripotent stem cell-derived bioartificial cardiac tissue cultivated under control conditions (left) or with G-stretch (right; notably both groups without AA). G-stretched bioartificial cardiac tissue showed large areas with uniform distribution of viable cardiomyocytes and better alignment along the longitudinal axis of the bioartificial cardiac tissue. Scale bars: 20 μm. (*B*) Transmission electron microscopy showed improved sarcomeric organization within CMs on d21 (symbols indicate sarcomere orientation) in cross-sections of G-stretched bioartificial cardiac tissue. Scale bars: 1 μm. (*C*) Immuno-fluorescence staining against cTnT (green) shows broader sarcomeric structures of G-stretched bioartificial cardiac tissue. Scale bars: 20 μm. (A) and (C) Nuclei stained with DAPI (blue). See also Supplementary material online, *Figures S4 and S5*.

Ascorbic acid affects murine induced pluripotent stem cell-derived bioartificial cardiac tissue morphology and contractility via changes in extracellular matrix organization

Ascorbic acid-treated BCTs showed areas with enhanced sarcomeric organization (*Figure 2A*) and more CM–CM contacts (intercalated discs; *Figure 2B*). Contraction forces at L_{max} were significantly higher compared with controls (0.97 ± 0.08 vs. 0.62 ± 0.03 mN on d14 and 1.15 ± 0.11 vs. 0.75 ± 0.06 mN on d21) (*Figure 3A*), with a clear Frank–Starling mechanism visible in the force–preload relation and a significant impact of AA already at preload ≥0.3 mm (see Supplementary material online, *Figure S4A*). In terms of passive forces (stiffness), BCTs treated with AA showed significantly higher values on d14 (7.36 ± 1.35 vs. 2.94 ± 0.51 mN) and d21 (9.53 ± 1.35 vs. 3.78 ± 0.65 mN) compared with untreated controls, both when determined at L_{max} (*Figure 3B*) and in force–preload measurements, also for AA-treated control constructs prepared from fibroblasts only (see Supplementary material online, *Figure S4B*). At the same time, the contraction frequency was slightly reduced, without differences in BCT cross-sectional area after treatment (see Supplementary material online, *Figure S4G and H*). Ascorbic acid-treated BCTs displayed elevated collagen deposition (*Figure 2C and D*) with significantly increased collagen I fibre width (21.1 ± 0.9 vs. 11.0 ± 0.4 μm, *Figure 3C*) and enhanced fibre alignment compared with controls on d21 (*Figure 3D*). Numbers of nuclei were also increased in the AA-treated BCT groups (*Figure 3E*), as well as TMRM intensities, measured on d21 (*Figure 3F*), and titin intensities of stained CMs in longitudinal sections of BCTs (*Figure 3G*). Sarcomere length was not affected by AA treatment (*Figure 3H*).

Application of growing stretch affects murine induced pluripotent stem cell-derived bioartificial cardiac tissue morphology and contractility via improved alignment and cellular maturation including sarcomere length changes

Common protocols for mechanical stimulation of artificial cardiac tissue employ cyclic uniaxial stretch (5–10%, 1–2 Hz).[7,27,31,34,37] Applied to our CB-based tissue constructs together with AA, cyclic stretch (10%; 1 Hz) for 7 days neither improved tissue morphology nor increased active forces [0.77 ± 0.07 mN ($n = 5$)

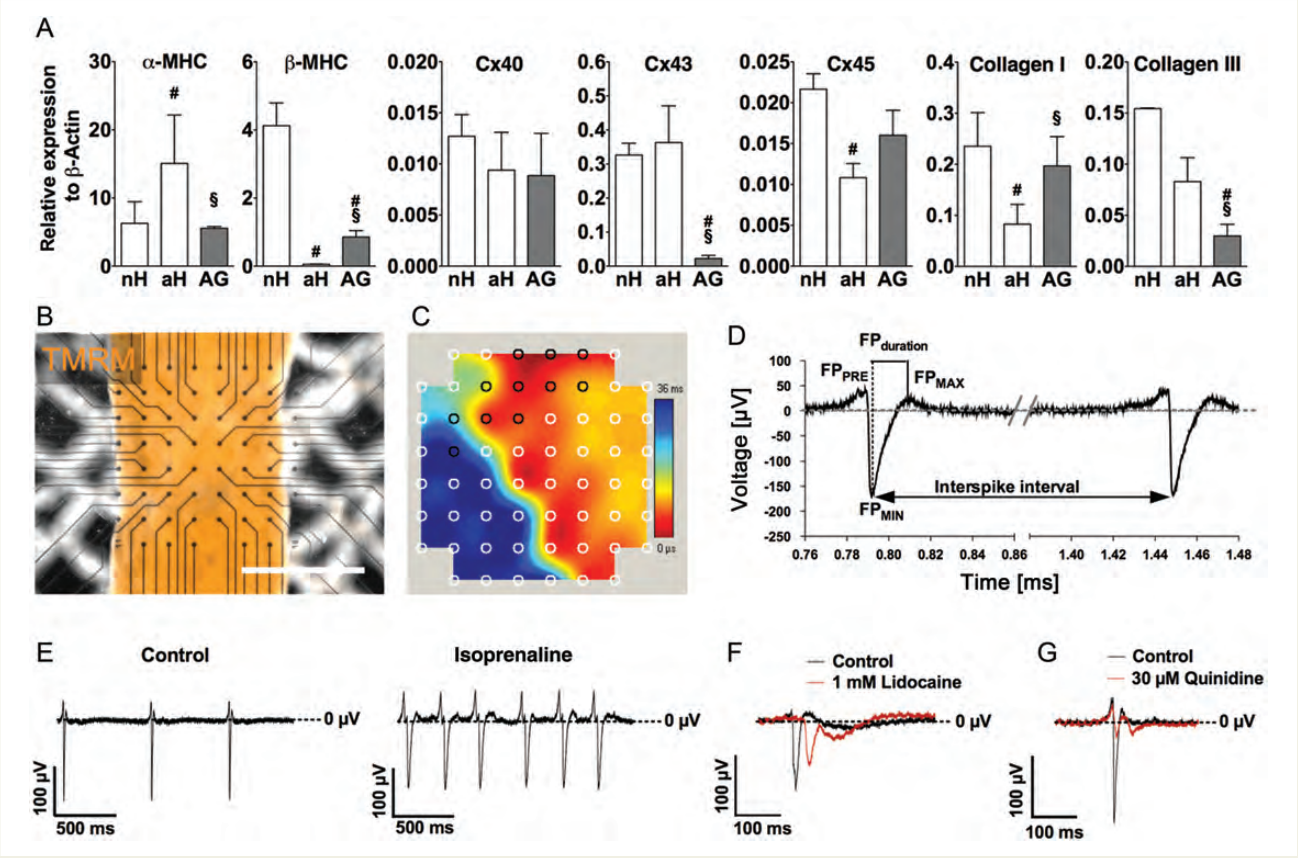

Figure 5 Gene expression and electrophysiology of optimized murine induced pluripotent stem cell-derived bioartificial cardiac tissue. (*A*) Quantitative real-time polymerase chain reaction analysis of optimized murine induced pluripotent stem cell-derived bioartificial cardiac tissue on d21 after combined ascorbic acid and G-stretch treatment demonstrated α-myosin heavy-chain, Cx40, Cx45, and collagen type I expression levels comparable with neonatal mouse heart (nH). Levels of Cx43 and β-myosin heavy chain were significantly lower than in neonatal mouse heart and argue for a rather embryonic phenotype; also, collagen type III levels were lower than in the heart; adult mouse heart (aH) shown for comparison; mean ± SD from $n = 4–6$ with polymerase chain reaction performed in triplicate; $^{\#}P \leq 0.05$ to nH; $^{\S}P \leq 0.05$ to aH; one-way analysis of variance. (*B*) A TMRM-labelled murine induced pluripotent stem cell-derived bioartificial cardiac tissue (d21) was plated on a micro-electrode array; scale bar: 1 mm. (*C*) Spatio-temporal colour-mapping showed the excitation propagation delay in the tissue during spontaneous contraction. (*D*) Cardiomyocyte-representative field potential recordings were obtained, and administration of 10 µM isoprenaline (*E*), 1 mM lidocaine (*F*), and 30 µM quinidine (*G*) demonstrated physiological drug responsiveness in murine induced pluripotent stem cell-derived bioartificial cardiac tissue.

vs. 0.97 ± 0.08 mN for static stretch ($n = 8$)] (see Supplementary material online, *Figure S4J and K*).

In an attempt to recapitulate the increasing systolic and diastolic pressure in the developing embryonic heart,[38] growing static stretch (G-stretch) was applied through stepwise elongation by 200 µm every second day from d7–d21, and led to an improved formation of elongated tissue from individual CBs (see Supplementary material online, *Figure S4J*). At the same time, large areas with uniform distribution of viable CMs and enhanced alignment along the longitudinal axis of the BCT (*Figure 4A*) were observed, together with improved sarcomeric organization within CMs on d21 (*Figure 4B*).

Application of G-stretch improved maximum contraction force development on d14 and d21, albeit to a lesser extent than in the AA-treated group (*Figure 3A* and see Supplementary material online, *Figure S4C*). In contrast, passive forces of stretched BCTs were higher compared with the controls and AA-treated BCTs (*Figure 3B* and see Supplementary material online, *Figure S4D*). Again, responses to preload in G-stretched CB-based constructs were recapitulated in G-stretched CM-free fibroblast-based constructs (see Supplementary material online, *Figure S4D*). Notably, higher forces observed after mechanical stimulation with G-stretch did not result in elevated gene expression levels for β-MHC, atrial natriuretic factor (ANF), brain natriuretic peptide, and α-skeletal actin (Act1a), which are usually associated with a hypertrophic response[39] (see Supplementary material online, *Figure S4L*). G-stretch resulted in increased collagen I fibre width in treated constructs, but to a lesser extent as in the AA-treated group (*Figure 3C*); an increase in collagen I fibre alignment was also detected, although not significant (*Figure 3D*). Nuclei

numbers remained unchanged (*Figure 3E*), but TMRM intensity and titin expression on d21 were significantly higher compared with the controls (*Figure 3F and G*). Moreover, and in contrast to AA-supplementation, treatment with G-stretch resulted in significantly increased sarcomere lengths within BCTs (*Figures 3H* and *4C*).

Combined ascorbic acid treatment and G-stretch lead to functionally optimized murine induced pluripotent stem cell-derived bioartificial cardiac tissue

Active contraction forces measured on d14 and d21 showed that combined treatment with AA and G-stretch during cultivation had an additional effect on mechanical properties of BCTs, compared with the untreated control and groups receiving individual treatment only, and resulted in forces of 1.22 ± 0.13 on d14 and 1.42 ± 0.09 mN on d21 (*Figure 3A*), again with a physiological force–preload relationship (see Supplementary material online, *Figure S4E*). Compared with untreated controls, on d21, maximum active forces almost doubled and passive forces were about three times higher when measured at L_{max} (*Figure 3B* and see Supplementary material online, *Figure S4F*). Murine iPSC-derived BCT functionality was analysed for up to 5 weeks in culture, with active forces of 1.27 ± 0.20 mN on d35 ($n = 3$). Combined treatment also led to highest passive forces in fibroblast-only constructs (see Supplementary material online, *Figure S4F*).

Combination of both stimuli reflected morphological changes in constructs treated with one stimulus only. Throughout the whole tissue, viable CMs were detectable using TMRM labelling during cultivation, as well as after immuno-staining for titin using mid-plane cryosections of BCTs (see Supplementary material online, *Figure S5A and B*). Broad, well-organized, and longitudinally aligned CM bundles were abundant (comparable with the stretched BCT group), staining positive for titin, cardiac troponin T, and MLC2v (see Supplementary material online, *Figure S5C–E*). Collagen I fibres were of comparable width as observed in the group treated with AA (*Figure 3C*), but showed further increased collagen I alignment (*Figure 3D*). Numbers of nuclei were comparable with the BCT group treated with AA, only (*Figure 3E*), while metabolic activity visualized by TMRM, titin intensities, and sarcomere length were comparable with those treated with G-stretch, only (*Figure 3F–H*). Optimized murine iPSC-derived BCTs after combined AA-treatment and G-stretch showed expression levels of α-MHC, Cx40, Cx45, and collagen type I comparable with neonatal mouse hearts (*Figure 5A*). In contrast, levels of β-MHC and collagen type III were significantly lower than in neonatal heart, as well as Cx43, which was expressed about 10-fold less. Despite this finding, optimized BCTs displayed synchronized spontaneous contractions (see Supplementary material online, *Movie S2*) and efficient CM coupling was demonstrated using microelectrode-array (MEA) measurement of whole-mounted BCTs (*Figure 5B*). We detected a propagation delay over the whole array (*Figure 5C*) at a conduction velocity of 2–3 cm/s, with CM-characteristic field potential (FP) recordings (*Figure 5D*); moreover, tissue constructs responded to cardiotropic drugs such as isoprenaline, lidocaine, and quinidine in a physiological manner (*Figure 5E–G*).

Human embryonic stem cell- and induced pluripotent stem cell-derived cardiac bodies form bioartificial cardiac tissue with functional characteristics resembling native myocardium

We generated transgenic human PSC lines expressing a neomycin resistance under control of the α-MHC promoter, which led to the generation of spontaneously beating human CBs (see Supplementary material online, *Figure S6A–D* and *Movie S3*). Notably, human CBs displayed a CM content of 100%, as after seeding of single cells dissociated from human CBs, immuno-staining confirmed every one of these cells to be cTnT-positive (see Supplementary material online, *Figure S6E and F*). Using our Matrigel™/collagen-based protocol with optimized conditions, i.e. addition of human foreskin fibroblasts, AA-supplementation, and G-stretch, human CBs efficiently fused into BCTs (see Supplementary material online, *Figure S7A*).

Human ESC-derived BCTs showed significant compaction during cultivation resulting in thin tissue bands with a cross-sectional area of 0.31 ± 0.11 mm^2 on d21 (see Supplementary material online, *Figure S7B*). Both human ESC-derived and human iPSC-derived BCTs showed longitudinal alignment of CMs and collagen bundles (*Figure 6A and B*) with viable CMs throughout the whole construct (see Supplementary material online, *Figure S8A*). Within BCTs, human stem cell-derived CMs expressed Nkx2.5 and Cx43 (*Figure 6C and D*); they displayed clear cross-striation and alignment of sarcomers (see Supplementary material online, *Figure S7J and K*). Besides the relatively mature phenotype observed for most CM within BCTs, some cells remain active in the cell cycle as shown by confocal microscopy analysis of immuno-staining for 2.5% Ki-67$^+$/Nkx2.5$^+$ CM within human iPSC-derived BCTs (see Supplementary material online, *Figure S9A*), and 3.6 ± 0.6% Ki-67$^+$/Nkx2.5$^+$ CM in human ESC-derived BCTs (not shown). Importantly, we did not observe residual expression of the pluripotency marker Oct3/4 in human ESC-derived BCTs. In contrast, BCTs showed strong expression of cardiac markers Nkx2.5, ANF, MLC2v, cTnT, α-MHC, and β-MHC, as well as CM-specific ion-channel proteins human Ether-à-go-go Related Gene, SCN5A, and CACNA1C, both on d8 and d22 (see Supplementary material online, *Figure S6G*). For optimized human ESC-derived BCTs after combined AA and G-stretch treatment, quantitative real-time PCR analysis demonstrated increasing expression levels of the ventricular myosin light-chain isoform MLC2v (in relation to MLC2a) and the ion-channel subunit Kir2.1 (mediating the inward rectifier potassium current I_{K1}), while levels of the ANF did not change significantly over time (*Figure 7A–C*). Spontaneous contractions were observed both in human iPSC- and human ESC-derived BCTs (see Supplementary material online, *Movie S4*), the latter with a frequency of up to 54.4 ± 3.6 bpm on d21 after combined treatment with AA and G-stretch (see Supplementary material online, *Figure S7G*). Efficient CM coupling was demonstrated using MEA measurement of whole-mounted BCTs (*Figure 7D*) with a conduction velocity of up to 4.9 cm/s. MEA

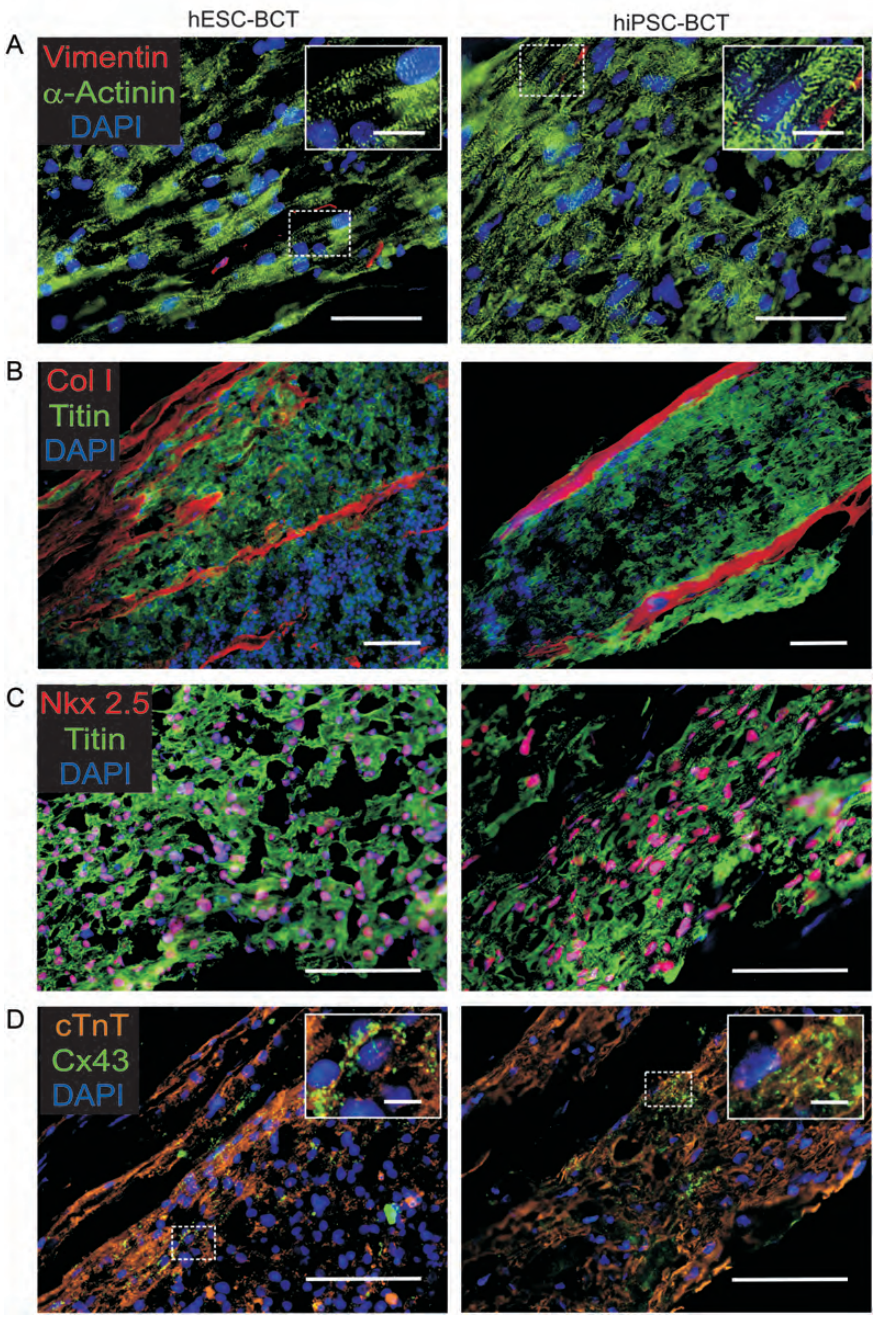

Figure 6 Human pluripotent stem cell-derived bioartificial cardiac tissue shows high density of cardiomyocytes and well-structured tissue morphology. (*A*) Both in sections of human embryonic stem cell-derived and human induced pluripotent stem cell-derived bioartificial cardiac tissue cultivated with ascorbic acid and G-stretch, longitudinally arranged (anisotropic) cardiomyocytes with distinct cross-striation were detected by immuno-fluorescence staining against α-sarcomeric actinin (green)/vimentin (red) on d21 and d28, respectively. (*B*) Both displayed similar cell and matrix organization with longitudinal alignment of collagen type I bundles (red) and cardiomyocytes visualized by staining titin (green). (*C*) Bioartificial cardiac tissue displayed a high density of viable cardiomyocytes staining positive for Nkx2.5 (red)/titin (green); (*D*) with expression of Cx43 (green) localized between cardiomyocytes (positive for cTnT, red). Nuclei stained with DAPI (blue); scale bars: (A) 50 μm, (B), (C), and (D) 100 μm; for insets=10 μm. See also Supplementary material online, *Figures S7 and S8*.

recordings showed an increase in contraction frequency in response to the β-adrenergic agonist isoprenaline (*Figure 7E*), which was quantified in bioreactor measurements of BCT contractility at a low Ca^{2+} concentration of 0.6 mM, demonstrating significantly increased frequencies of 199 ± 51% of baseline levels (*Figure 7F*). Moreover, following isoprenaline addition, active forces

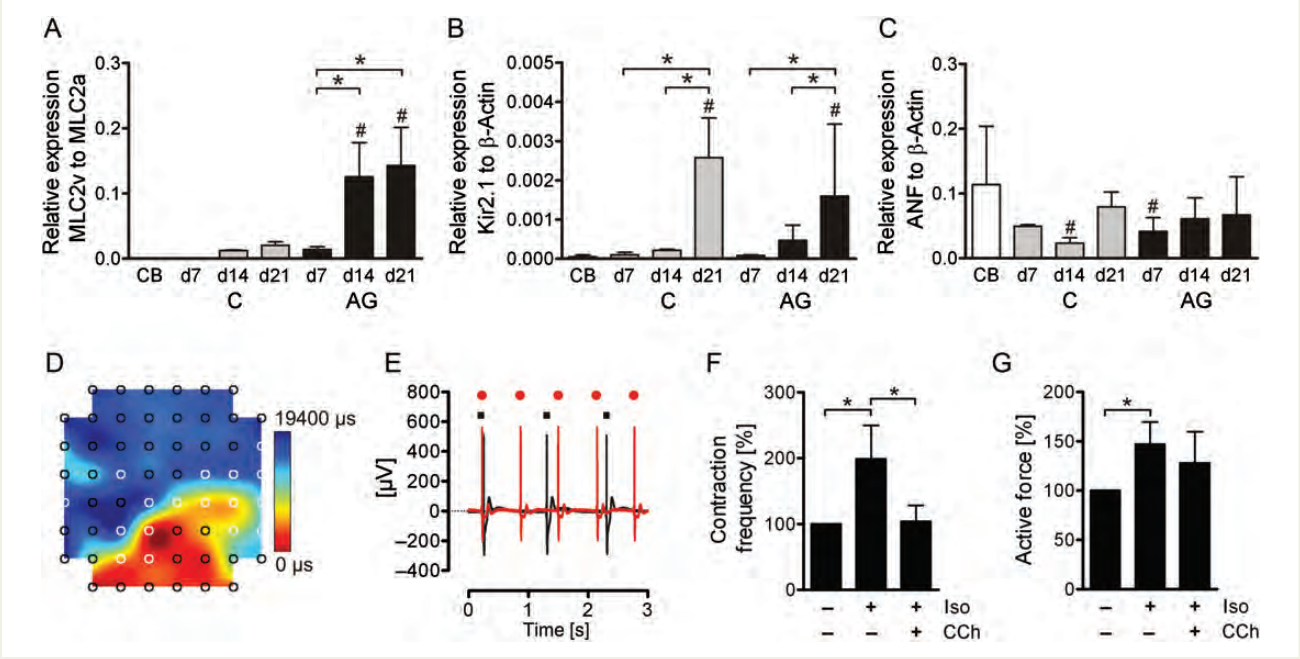

Figure 7 Optimized human pluripotent stem cell-derived bioartificial cardiac tissue show maturation towards a ventricular phenotype. Quantitative real-time polymerase chain reaction analysis of optimized human embryonic stem cell-derived bioartificial cardiac tissue on d7, d14, and d21 showed (*A*) increasing expression levels of the ventricular myosin light-chain isoform MLC2v in relation to MLC2a after combined ascorbic acid and G-stretch treatment (AG, black bars) but not in untreated controls (C, grey bars), and (*B*) increasing expression levels of Kir2.1 in both groups over time, while (*C*) expression levels of atrial natriuretic factor did not change significantly. Expression levels of human cardiac bodies on d23 of differentiation are shown for comparison, representing the starting material for bioartificial cardiac tissue preparation; mean ± SD ($n = 3$ with polymerase chain reaction performed in triplicate; $^{\#}P \leq 0.05$ to cardiac bodies; $^{*}P \leq 0.05$ between indicated groups). (*D*) Microelectrode array-based spatio-temporal colour mapping showed the excitation propagation delay in the tissue during spontaneous contraction of a human embryonic stem cell-derived bioartificial cardiac tissue on d22. (*E*) Cardiomyocyte-representative field potential recordings were obtained (black, see squares), and administration of 10 µM isoprenaline demonstrated physiological drug responsiveness (red, see circles). See also Supplementary material online, *Movie S4*. Noradrenaline was added between d7 and d21 to all ascorbic acid and G-stretch-treated Matrigel™-bioartificial cardiac tissue. Functionality of human embryonic stem cell-derived bioartificial cardiac tissue was further demonstrated by assessment of spontaneous contraction frequencies (F) and active forces (G), both at 0.6 mM Ca^{2+} and in response to 0.1 µM isoprenaline (Iso) and 10 µM carbachol (CCh); values are given normalized to un-stimulated baseline levels (=100%) as mean ± SD for $n = 6$; $^{*}P \leq 0.05$; one-way analysis of variance.

were significantly increased to 147 ± 22% (*Figure 7G*). Subsequent addition of the muscarinergic agonist carbachol (10 µM) reduced both contraction frequency and active forces (*Figure 7F and G*).

Functionality of human iPSC-derived and human ESC-derived BCTs was further demonstrated by the assessment of active and passive forces in response to increasing preload (*Figure 8A and B*). For d21 human ESC-derived BCTs, combined AA-supplementation and G-stretch resulted in higher maximum active forces of 1.37 ± 0.18 vs. 0.78 ± 0.17 mN for the untreated control (*Figure 8C and E*). Passive forces were significantly increased on d14 (8.50 ± 1.71 vs. 3.30 ± 1.54 mN), both when determined at L_{max} (*Figure 8D*) and in force–preload measurements (*Figure 8F*), and tended to be higher on d21, although not reaching statistical significance (4.66 ± 0.64 vs. 1.57 ± 0.52 mN). In addition, to replace the undefined animal-derived Matrigel™, we used a defined matrix (DM) for human BCTs, which is based on human collagen type I and *in situ* cross-linking hyaluronic acid hydrogel and devoid of any animal-derived components (Dahlmann *et al.*, in press).[35] Using optimized conditions for tissue preparation and maturation, our DM–BCTs yielded similar forces per construct as observed using Matrigel™ (see Supplementary material online, *Figure S7C–F and L*). Finally, details of an original force recording of a human iPSC-derived BCT are presented in Supplementary material online, *Figure S9B–D*.

Discussion

In this study, we demonstrate rigorous purification of PSC-derived CMs with transgene-based antibiotic selection.[27,29] We describe for the first time that pure CMs in autonomously contracting highly defined units, i.e. CBs, can be used directly, i.e. without harmful disruption of pre-formed functional cell–cell contacts, for the generation of three-dimensional BCT with physiological properties. In our hands, the use of Zeocin™ selection-based single cell-dissociated murine iPSC–CMs sparsely led to contracting tissue with reduced cell viability and active forces.

As indicated by the connexin expression pattern, our CBs have to be considered as artificial three-dimensional monocultures of pure CMs at an early developmental stage. We hypothesized

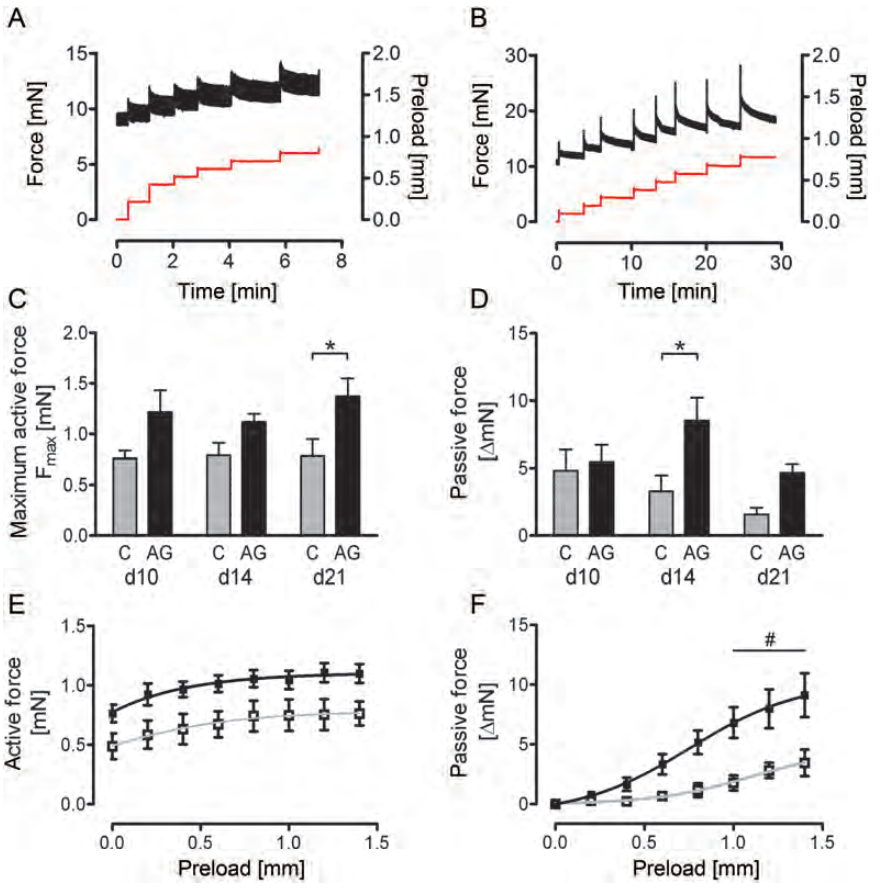

Figure 8 Optimized human pluripotent stem cell-derived bioartificial cardiac tissue shows increased active and passive contraction forces. Functionality of human induced pluripotent stem cell-derived (*A*) and human embryonic stem cell-derived bioartificial cardiac tissue (*B*) was demonstrated by assessment of active and passive contraction forces upon electrical pacing in response to increasing preload at d28 and d21, respectively. (*C*) Maximum contraction forces of human embryonic stem cell-derived bioartificial cardiac tissue from different treatment groups: C, control, and AG, ascorbic acid and G-stretch, measured after electrical pacing (25 V, 10 ms) showed increased forces after the combined treatment on d10, d14, and d21. (*D*) With AG-treatment, human embryonic stem cell-derived bioartificial cardiac tissue passive forces increased over time from d10 to d14, and were significantly higher than in untreated controls. (*E*) Preload was increased stepwise to determine maximum active force (F_{max}) for human embryonic stem cell-derived bioartificial cardiac tissue treated with AG (full squares), compared with untreated controls (open squares) on d14; both curves reflect the Frank–Starling mechanism of increasing force–preload relation seen in native heart muscle. (*F*) Similarly, d14 passive force–preload relation in human embryonic stem cell-derived bioartificial cardiac tissue was significantly higher in the AG group (full squares) vs. controls (open squares). Symbols represent mean baseline force ± SEM; (C) and (D) $n = 3–7$ per group; (E) and (F) $n = 4–7$ per group. $^{*}P \leq 0.05$ between indicated groups; $^{\#}P \leq 0.05$ for all indicated data points compared with respective control at the same preload. See also Supplementary material online, *Figures S7 and S9*.

that these immature myocytes, just like in the embryonic heart, may display a high degree of plasticity and migratory capacity to enable CB fusion and substantial remodelling towards structural and functional homogenous cardiac tissue. Indeed, CB fusion resulted in a functional syncytium. Notably, the direct use of undissociated CBs was possible only because the EB-based selection procedure was optimized to eliminate any residual Oct3/4-eGFP^{+} PSCs in CBs and BCTs, thus preventing the formation of disorganized non-cardiac tissue components typically observed using non-selected EBs.

In situ characterization of CB-based murine iPSC-derived BCTs in a bioreactor for 21 days allowed us to identify critical effectors of tissue formation and functionality and their mechanisms of action. It has been reported for isolated primary rat heart cells[7] and dissociated murine ESC-derived CMs that the presence of a certain proportion of fibroblasts is essential for cell alignment[40] and the generation of engineered heart tissue.[29] We could confirm these findings for murine iPSC-derived CMs. Moreover, we now demonstrate that fibroblast-driven ECM formation and remodelling does not only support interconnection of adjacent individual myocytes. As suggested by Supplementary material online *Movie S1*, it was also essential to overcome the functional and structural isolation of initially distant CBs, and was required for final fusion of individual CBs into homogenous and stable BCTs with considerably higher forces.

As a further measure to improve functionality of iPSC–BCTs, we evaluated medium supplementation with AA. Ascorbic acid is well known for its radical scavenger properties and regulatory effects both on pro-collagen expression and collagen post-transcriptional modification.[41] It can also act as a pro-oxidant in differentiating mouse ESCs[42] and improve cardiac differentiation and maturation as well as CM progenitor cell proliferation.[43] In addition to the positive effect of AA on ECM and cellular organization within BCTs, our data provide evidence for direct effects on CM maturation or survival. This was demonstrated by increased collagen fibre width and alignment, adding to the passive forces, as well as higher nuclei numbers, metabolic activity, and titin protein levels of CMs, altogether resulting in higher active contraction and passive forces for AA-treated BCTs.

Another critical factor for tissue functionality identified in this study is increasing mechanical stimulation. Common protocols for mechanical stimulation of artificial cardiac tissue use invariant cyclic uni-axial stretch (5–10%, 1–2 Hz), which is usually accompanied by a hypertrophic response.[7,25,27,34] While uni-axial cyclic stretch might interfere with spontaneous isotropic contractions of early CMs within CBs, growing uniform stretch could be beneficial to recapitulate the physiological conditions of the growing embryonic myocardium with increasing systolic and diastolic pressure[37] and continuously increasing contractile force.[44] Growing static stretch has been shown to induce rabbit skeletal muscle growth *in vivo*;[45] however, it has not been applied in cardiac tissue engineering before.

In our study, mechanical stimulation with growing static stretch led to significantly higher forces when compared with invariant cyclic stretch and consequently was used in all further experiments. On a structural level, G-stretch had a significant impact on CM viability and metabolism as demonstrated by increased TMRM fluorescence. It induced improved sarcomere alignment and increased sarcomere length within stretched BCTs. This is similar to embryonic heart development; here, an increase in myofibre density and improvement in the alignment of myocytes was described as additional underlying mechanisms of an increase in contraction forces, which cannot be ascribed to the accumulation of contractile proteins (MHC) only.[44] Also, in heart development, regional myofibre alignment is observed preferentially at sites of regional orthotropic epicardial wall strain[46] and higher forces from aligned tissue generated *in vitro* have been demonstrated.[47]

The above positive effects of fibroblast addition, AA supplementation, and growing mechanical stretch were successfully combined for optimized murine iPSC-derived BCTs with improved functionality. The molecular mechanisms supporting increased force development most probably involve a positive feedback loop of cell-mediated matrix synthesis, remodelling, and organization on the one hand, and matrix-mediated effects on cellular viability, metabolism, ultra-structure and contractility on the other hand, as proposed by Discher *et al.*[48] Although Cx43 expression levels in these optimized BCTs were significantly lower than in the native heart, MEA measurement demonstrated efficient coupling, presumably with a major contribution of Cx45 gap junctions, leading to synchronized contractions of whole BCTs.

Our data demonstrate that this novel approach can be extended to human iPSCs and ESCs for the *in vitro* generation of well-structured myocardial-like tissue. Moreover, as CM maturation can be assessed based on the expression level of MLC2v[49] and Kir2.1,[50,51] we conclude that our optimized human ESC-derived BCTs showed maturation towards a ventricular phenotype. Functionality was demonstrated both for murine and human BCTs by direct force measurement. So far, no data have been available on the contraction forces of murine iPSC-derived BCT. However, active forces for murine iPSC–BCTs obtained with our novel CB-based protocols are of the same magnitude as achieved by state-of-the-art cardiac tissue engineered constructs based on isolated primary neonatal rat CMs using similar cell numbers per volume[7,34,52] or murine ESC-derived CMs.[29]

With active contraction forces of the BCT of up to 1.37 ± 0.18 mN at a cross-sectional area of 0.31 ± 0.11 mm^2 on d21, our human BCTs reached a maximum active tension of 4.4 mN/mm^2. Notably, this is 37- and 55-fold higher than reported recently for human ESC-derived tissue generated from non-enriched[23] or partially enriched CMs,[31] respectively. These data clearly confirm the need for vigorous CM purification. Human DM–BCTs based on human collagen type I and hyaluronic acid, which are devoid of any animal-derived components, displayed active contraction forces comparable with Matrigel^{TM}-based constructs.

Active contraction forces of myocardial strips isolated from native human ventricles have been determined to range between 14.5 ± 4.4 and 22.8 ± 1.4 mN/mm^2 for healthy donors.[53,54] Therefore, maximum forces of our human BCTs are only 3- to 5-fold lower than active forces reported for native human myocardium.

Human BCT contractility was modulated in response to isoprenaline with a positive chronotropic effect and in response to carbachol with a negative chronotropic effect, demonstrating functional β-adrenergic and muscarinergic receptor systems.[23] For our optimized human BCTs, these effects were even more pronounced than demonstrated before for human PSC-derived CMs[55] and engineered heart tissue.[23] Moreover, we were able to show a significant positive inotropic effect of isoprenaline on human BCTs, arguing in favour of the existence of a functional sarcoplasmic reticulum, which is a hallmark of mature myocardium.[56] This inotropic effect was absent or found less pronounced in previous studies on human PSC-derived CMs[55] or engineered heart tissue,[23] respectively.

We conclude that highly efficient enrichment of murine and human PSC-derived CMs in CBs allowed for successful cardiac tissue formation and maturation, with so far unparalleled contraction forces. Cardiac tissue patches with improved functionality should be valuable for high throughput pharmacological testing and iPSC-based cardiac disease modelling.[57] They provide reproducible three-dimensional cell culture models, and in combination with suitable read-out systems such as our miniaturized multimodal bioreactor, they enable the investigation of certain mechanistic aspects of disease and regeneration already *in vitro*. For future clinical application, genetic selection of PSC-derived CMs needs to be further optimized; in this regard, the use of zinc-finger nucleases, which have been designed to target 'safe harbour sites' such as the adeno-associated virus integration site 1 locus in human ESCs and iPSCs,[58] appears to be a promising approach for controlled and safe insertion of selection markers.

Alternatively, the recently described FACS sorting using surface markers such as signal regulatory protein alpha might offer a non-genetic CM selection strategy.[59] Moreover, for future clinical application, it might soon be possible to address the problem of insufficient vascularization of *in vitro* generated working myocardium through the application of MSCs, as proposed by Tulloch et *al.*,[31] or more likely, cardiovascular progenitor cell types selectable from iPSCs as shown by Mauritz et *al.*[18] Recently, Zwi-Dantsis *et al.*[5] demonstrated the generation of functional CMs even from advanced heart failure patients' iPSCs. Now, our advanced protocols yielded human PSC-derived BCT with contractile forces comparable with native myocardium. In addition, our study demonstrated the implementation of a defined animal-free matrix based on pure human collagen and hyaluronic acid and therefore might represent a major step towards clinical applicability of stem cell-based engineered heart tissue for myocardial repair.

Supplementary material

Supplementary material is available at *European Heart Journal* online.

Acknowledgements

We thank Hans Schöler and Holm Zähres for providing OG2-iPS cells, Monica Jara Avaca for the characterization of clonal lines thereof, and Lena Möller for the production of cross-linkable hyaluronic acid. We are thankful to Matthias Ballmeier for excellent assistance in FACSorting, to Virginija Jazbutyte for contributing RNA samples, and to Joerg Heineke for primer sequences and helpful discussion.

Funding

This work was funded by the Cluster of Excellence REBIRTH (DFG EXC 62/1), by the German Ministry for Education and Science (BMBF, 01GN0958), and by the Cortiss foundation.

Conflict of interest: none declared.

References

1. Hassink RJ, Pasumarthi KB, Nakajima H, Rubart M, Soonpaa MH, de la Riviere AB, Doevendans PA, Field LJ. Cardiomyocyte cell cycle activation improves cardiac function after myocardial infarction. *Cardiovasc Res* 2008;**78**:18–25.
2. Porrello ER, Mahmoud AI, Simpson E, Hill JA, Richardson JA, Olson EN, Sadek HA. Transient regenerative potential of the neonatal mouse heart. *Science* 2011;**331**:1078–1080.
3. Laflamme MA, Chen KY, Naumova AV, Muskheli V, Fugate JA, Dupras SK, Reinecke H, Xu C, Hassanipour M, Police S, O'Sullivan C, Collins L, Chen Y, Minami E, Gill EA, Ueno S, Yuan C, Gold J, Murry CE. Cardiomyocytes derived from human embryonic stem cells in pro-survival factors enhance function of infarcted rat hearts. *Nat Biotechnol* 2007;**25**:1015–1024.
4. Caspi O, Huber I, Kehat I, Habib M, Arbel G, Gepstein A, Yankelson L, Aronson D, Beyar R, Gepstein L. Transplantation of human embryonic stem cell-derived cardiomyocytes improves myocardial performance in infarcted rat hearts. *J Am Coll Cardiol* 2007;**50**:1884–1893.
5. Zwi-Dantsis L, Huber I, Habib M, Winterstern A, Gepstein A, Arbel G, Gepstein L. Derivation and cardiomyocyte differentiation of induced pluripotent stem cells from heart failure patients. *Eur Heart J*. Advance Access published 2012, May 22, doi:10.1093/eurheartj/ehs096.
6. Zimmermann WH, Didie M, Wasmeier GH, Nixdorff U, Hess A, Melnychenko I, Boy O, Neuhuber WL, Weyand M, Eschenhagen T. Cardiac grafting of engineered heart tissue in syngenic rats. *Circulation* 2002;**106**(Suppl. 1):I151–157.
7. Naito H, Melnychenko I, Didie M, Schneiderbanger K, Schubert P, Rosenkranz S, Eschenhagen T, Zimmermann WH. Optimizing engineered heart tissue for therapeutic applications as surrogate heart muscle. *Circulation* 2006;**114**(Suppl.):I72–78.
8. Vunjak-Novakovic G, Tandon N, Godier A, Maidhof R, Marsano A, Martens TP, Radisic M. Challenges in cardiac tissue engineering. *Tissue Eng Part B Rev* 2010;**16**:169–187.
9. Kehat I, Kenyagin-Karsenti D, Snir M, Segev H, Amit M, Gepstein A, Livne E, Binah O, Itskovitz-Eldor J, Gepstein L. Human embryonic stem cells can differentiate into myocytes with structural and functional properties of cardiomyocytes. *J Clin Invest* 2001;**108**:407–414.
10. Schwanke K, Wunderlich S, Reppel M, Winkler ME, Matzkies M, Groos S, Itskovitz-Eldor J, Simon AR, Hescheler J, Haverich A, Martin U. Generation and characterization of functional cardiomyocytes from rhesus monkey embryonic stem cells. *Stem Cells* 2006;**24**:1423–1432.
11. Takahashi K, Yamanaka S. Induction of pluripotent stem cells from mouse embryonic and adult fibroblast cultures by defined factors. *Cell* 2006;**126**:663–676.
12. Nakagawa M, Koyanagi M, Tanabe K, Takahashi K, Ichisaka T, Aoi T, Okita K, Mochiduki Y, Takizawa N, Yamanaka S. Generation of induced pluripotent stem cells without Myc from mouse and human fibroblasts. *Nat Biotechnol* 2008;**26**:101–106.
13. Schenke-Layland K, Rhodes KE, Angelis E, Butylkova Y, Heydarkhan-Hagvall S, Gekas C, Zhang R, Goldhaber JI, Mikkola HK, Plath K, MacLellan WR. Reprogrammed mouse fibroblasts differentiate into cells of the cardiovascular and hematopoietic lineages. *Stem Cells* 2008;**26**:1537–1546.
14. Mauritz C, Schwanke K, Reppel M, Neef S, Katsirntaki K, Maier LS, Nguemo F, Menke S, Haustein M, Hescheler J, Hasenfuss G, Martin U. Generation of functional murine cardiac myocytes from induced pluripotent stem cells. *Circulation* 2008;**118**:507–517.
15. Narazaki G, Uosaki H, Teranishi M, Okita K, Kim B, Matsuoka S, Yamanaka S, Yamashita JK. Directed and systematic differentiation of cardiovascular cells from mouse induced pluripotent stem cells. *Circulation* 2008;**118**:498–506.
16. Haase A, Olmer R, Schwanke K, Wunderlich S, Merkert S, Hess C, Zweigerdt R, Gruh I, Meyer J, Wagner S, Maier LS, Han DW, Glage S, Miller K, Fischer P, Scholer HR, Martin U. Generation of induced pluripotent stem cells from human cord blood. *Cell Stem Cell* 2009;**5**:434–441.
17. Warren L, Manos PD, Ahfeldt T, Loh YH, Li H, Lau F, Ebina W, Mandal PK, Smith ZD, Meissner A, Daley GQ, Brack AS, Collins JJ, Cowan C, Schlaeger TM, Rossi DJ. Highly efficient reprogramming to pluripotency and directed differentiation of human cells with synthetic modified mRNA. *Cell Stem Cell* 2010;**7**:618–630.
18. Mauritz C, Martens A, Rojas SV, Schnick T, Rathert C, Schecker N, Menke S, Glage S, Zweigerdt R, Haverich A, Martin U, Kutschka I. Induced pluripotent stem cell (iPSC)-derived Flk-1 progenitor cells engraft, differentiate, and improve heart function in a mouse model of acute myocardial infarction. *Eur Heart J* 2011;**32**:2634–2641.
19. Nelson TJ, Martinez-Fernandez A, Yamada S, Perez-Terzic C, Ikeda Y, Terzic A. Repair of acute myocardial infarction by human stemness factors induced pluripotent stem cells. *Circulation* 2009;**120**:408–416.
20. Xue T, Cho HC, Akar FG, Tsang SY, Jones SP, Marban E, Tomaselli GF, Li RA. Functional integration of electrically active cardiac derivatives from genetically engineered human embryonic stem cells with quiescent recipient ventricular cardiomyocytes: insights into the development of cell-based pacemakers. *Circulation* 2005;**111**:11–20.
21. Christoforou N, Oskouei BN, Esteso P, Hill CM, Zimmet JM, Bian W, Bursac N, Leong KW, Hare JM, Gearhart JD. Implantation of mouse embryonic stem cell-derived cardiac progenitor cells preserves function of infarcted murine hearts. *PLoS One* 2010;**5**:e11536.
22. van Laake LW, Passier R, den Ouden K, Schreurs C, Monshouwer-Kloots J, Ward-van Oostwaard D, van Echteld CJ, Doevendans PA, Mummery CL. Improvement of mouse cardiac function by hESC-derived cardiomyocytes correlates with vascularity but not graft size. *Stem Cell Res* 2009;**3**:106–112.
23. Schaaf S, Shibamiya A, Mewe M, Eder A, Stohr A, Hirt MN, Rau T, Zimmermann WH, Conradi L, Eschenhagen T, Hansen A. Human engineered heart tissue as a versatile tool in basic research and preclinical toxicology. *PLoS One* 2011;**6**:e26397.
24. Xu XQ, Graichen R, Soo SY, Balakrishnan T, Rahmat SN, Sieh S, Tham SC, Freund C, Moore J, Mummery C, Colman A, Zweigerdt R, Davidson BP. Chemically defined medium supporting cardiomyocyte differentiation of human embryonic stem cells. *Differentiation* 2008;**76**:958–970.
25. Guo XM, Zhao YS, Chang HX, Wang CY, E LL, Zhang XA, Duan CM, Dong LZ, Jiang H, Li J, Song Y, Yang XJ. Creation of engineered cardiac tissue in vitro from mouse embryonic stem cells. *Circulation* 2006;**113**:2229–2237.
26. Wang X, Wei G, Yu W, Zhao Y, Yu X, Ma X. Scalable producing embryoid bodies by rotary cell culture system and constructing engineered cardiac tissue with ES-derived cardiomyocytes in vitro. *Biotechnol Prog* 2006;**22**:811–818.
27. Shimko VF, Claycomb WC. Effect of mechanical loading on three-dimensional cultures of embryonic stem cell-derived cardiomyocytes. *Tissue Eng Part A* 2008;**14**:49–58.

28. Pfannkuche K, Neuss S, Pillekamp F, Frenzel LP, Attia W, Hannes T, Salber J, Hoss M, Zenke M, Fleischmann BK, Hescheler J, Saric T. Fibroblasts facilitate the engraftment of embryonic stem cell-derived cardiomyocytes on three-dimensional collagen matrices and aggregation in hanging drops. *Stem Cells Dev* 2010;**19**:1589–1599.
29. Liau B, Christoforou N, Leong KW, Bursac N. Pluripotent stem cell-derived cardiac tissue patch with advanced structure and function. *Biomaterials* 2011;**32**:9180–9187.
30. Matsuura K, Masuda S, Haraguchi Y, Yasuda N, Shimizu T, Hagiwara N, Zandstra PW, Okano T. Creation of mouse embryonic stem cell-derived cardiac cell sheets. *Biomaterials* 2011;**32**:7355–7362.
31. Tulloch NL, Muskheli V, Razumova MV, Korte FS, Regnier M, Hauch KD, Pabon L, Reinecke H, Murry CE. Growth of engineered human myocardium with mechanical loading and vascular coculture. *Circ Res* 2011;**109**:47–59.
32. Burridge PW, Thompson S, Millrod MA, Weinberg S, Yuan X, Peters A, Mahairaki V, Koliatsos VE, Tung L, Zambidis ET. A universal system for highly efficient cardiac differentiation of human induced pluripotent stem cells that eliminates interline variability. *PLoS One* 2011;**6**:e18293.
33. Zimmermann WH, Melnychenko I, Wasmeier G, Didie M, Naito H, Nixdorff U, Hess A, Budinsky L, Brune K, Michaelis B, Dhein S, Schwoerer A, Ehmke H, Eschenhagen T. Engineered heart tissue grafts improve systolic and diastolic function in infarcted rat hearts. *Nat Med* 2006;**12**:452–458.
34. Kensah G, Gruh I, Viering J, Schumann H, Dahlmann J, Meyer H, Skvorc D, Bar A, Akhyari P, Heisterkamp A, Haverich A, Martin U. A novel miniaturized multimodal bioreactor for continuous in situ assessment of bioartificial cardiac tissue during stimulation and maturation. *Tissue Eng C Methods* 2011;**17**:463–473.
35. Dahlmann J, Krause A, Möller L, Kensah G, Möwes M, Diekmann A, Martin U, Kirschning A, Gruh I, Dräger G. Fully defined in situ cross-linkable alginate and hyaluronic acid hydrogels for myocardial tissue engineering. *Biomaterials* in press.
36. Hattori F, Chen H, Yamashita H, Tohyama S, Satoh YS, Yuasa S, Li W, Yamakawa H, Tanaka T, Onitsuka T, Shimoji K, Ohno Y, Egashira T, Kaneda R, Murata M, Hidaka K, Morisaki T, Sasaki E, Suzuki T, Sano M, Makino S, Oikawa S, Fukuda K. Nongenetic method for purifying stem cell-derived cardiomyocytes. *Nat Methods* 2010;**7**:61–66.
37. Fink C, Ergun S, Kralisch D, Remmers U, Weil J, Eschenhagen T. Chronic stretch of engineered heart tissue induces hypertrophy and functional improvement. *FASEB J* 2000;**14**:669–679.
38. Ishiwata T, Nakazawa M, Pu WT, Tevosian SG, Izumo S. Developmental changes in ventricular diastolic function correlate with changes in ventricular myoarchitecture in normal mouse embryos. *Circ Res* 2003;**93**:857–865.
39. Tiburcy M, Didie M, Boy O, Christalla P, Doker S, Naito H, Karikkineth BC, El-Armouche A, Grimm M, Nose M, Eschenhagen T, Zieseniss A, Katschinksi DM, Hamdani N, Linke WA, Yin X, Mayr M, Zimmermann WH. Terminal differentiation, advanced organotypic maturation, and modeling of hypertrophic growth in engineered heart tissue. *Circ Res* 2011;**109**:1105–1114.
40. Parrag IC, Zandstra PW, Woodhouse KA. Fiber alignment and coculture with fibroblasts improves the differentiated phenotype of murine embryonic stem cell-derived cardiomyocytes for cardiac tissue engineering. *Biotechnol Bioeng* 2012;**109**:813–822.
41. Mandl J, Szarka A, Banhegyi G. Vitamin C: update on physiology and pharmacology. *Br J Pharmacol* 2009;**157**:1097–1110.
42. Crespo FL, Sobrado VR, Gomez L, Cervera AM, McCreath KJ. Mitochondrial reactive oxygen species mediate cardiomyocyte formation from embryonic stem cells in high glucose. *Stem Cells* 2010;**28**:1132–1142.
43. Cao N, Liu Z, Chen Z, Wang J, Chen T, Zhao X, Ma Y, Qin L, Kang J, Wei B, Wang L, Jin Y, Yang H-T. Ascorbic acid enhances the cardiac differentiation of induced pluripotent stem cells through promoting the proliferation of cardiac progenitor cells. *Cell Res* 2012;**22**:219–236.
44. Siedner S, Krüger M, Schroeter M, Metzler D, Roell W, Fleischmann BK, Hescheler J, Pfitzer G, Stehle R. Developmental changes in contractility and sarcomeric proteins from the early embryonic to the adult stage in the mouse heart. *J Physiol* 2003;**548**:493–505.
45. Cox VM, Williams PE, Wright H, James RS, Gillott KL, Young IS, Goldspink DF. Growth induced by incremental static stretch in adult rabbit latissimus dorsi muscle. *Exp Physiol* 2000;**85**:193–202.
46. Alford PW, Taber LA. Regional epicardial strain in the embryonic chick heart during the early looping stages. *J Biomech* 2003;**36**:1135–1141.
47. Black LD, Meyers JD, Weinbaum JS, Shvelidze YA, Tranquillo RT. Cell-induced alignment augments twitch force in fibrin gel-based engineered myocardium via gap junction modification. *Tissue Eng A* 2009;**15**:3099–3108.
48. Discher DE, Janmey P, Wang YL. Tissue cells feel and respond to the stiffness of their substrate. *Science* 2005;**310**:1139–1143.
49. Lian X, Hsiao C, Wilson G, Zhu K, Hazeltine LB, Azarin SM, Raval KK, Zhang J, Kamp TJ, Palecek SP. Robust cardiomyocyte differentiation from human pluripotent stem cells via temporal modulation of canonical Wnt signaling. *Proc Natl Acad Sci USA* 2012;**109**:E1848–1857.
50. Sartiani L, Bettiol E, Stillitano F, Mugelli A, Cerbai E, Jaconi ME. Developmental changes in cardiomyocytes differentiated from human embryonic stem cells: a molecular and electrophysiological approach. *Stem Cells* 2007;**25**:1136–1144.
51. Gaborit N, Le Bouter S, Szuts V, Varro A, Escande D, Nattel S, Demolombe S. Regional and tissue specific transcript signatures of ion channel genes in the non-diseased human heart. *J Physiol* 2007;**582**(Pt 2):675–693.
52. Eschenhagen T. The beat goes on: human heart muscle from pluripotent stem cells. *Circ Res* 2011;**109**:2–4.
53. Holubarsch C, Ludemann J, Wiessner S, Ruf T, Schulte-Baukloh H, Schmidt-Schweda S, Pieske B, Posival H, Just H. Shortening versus isometric contractions in isolated human failing and non-failing left ventricular myocardium: dependency of external work and force on muscle length, heart rate and inotropic stimulation. *Cardiovasc Res* 1998;**37**:46–57.
54. Mulieri LA, Hasenfuss G, Leavitt B, Allen PD, Alpert NR. Altered myocardial force-frequency relation in human heart failure. *Circulation* 1992;**85**:1743–1750.
55. Pillekamp F, Haustein M, Khalil M, Emmelheinz M, Nazzal R, Adelmann R, Nguemo F, Rubenchyk O, Pfannkuche K, Matzkies M, Reppel M, Bloch W, Brockmeier K, Hescheler J. Contractile properties of early human embryonic stem cell-derived cardiomyocytes: beta-adrenergic stimulation induces positive chronotropy and lusitropy but not inotropy. *Stem Cells Dev* 2012;**21**:2111–2121.
56. Dolnikov K, Shilkrut M, Zeevi-Levin N, Gerecht-Nir S, Amit M, Danon A, Itskovitz-Eldor J, Binah O. Functional properties of human embryonic stem cell-derived cardiomyocytes: intracellular Ca^{2+} handling and the role of sarcoplasmic reticulum in the contraction. *Stem Cells* 2006;**24**:236–245.
57. Moretti A, Bellin M, Welling A, Jung CB, Lam JT, Bott-Flugel L, Dorn T, Goedel A, Hohnke C, Hofmann F, Seyfarth M, Sinnecker D, Schomig A, Laugwitz KL. Patient-specific induced pluripotent stem-cell models for long-QT syndrome. *N Engl J Med* 2010;**363**:1397–1409.
58. Hockemeyer D, Soldner F, Beard C, Gao Q, Mitalipova M, DeKelver RC, Katibah GE, Amora R, Boydston EA, Zeitler B, Meng X, Miller JC, Zhang L, Rebar EJ, Gregory PD, Urnov FD, Jaenisch R. Efficient targeting of expressed and silent genes in human ESCs and iPSCs using zinc-finger nucleases. *Nat Biotechnol* 2009;**27**:851–857.
59. Dubois NC, Craft AM, Sharma P, Elliott DA, Stanley EG, Elefanty AG, Gramolini A, Keller G. SIRPA is a specific cell-surface marker for isolating cardiomyocytes derived from human pluripotent stem cells. *Nat Biotechnol* 2011;**29**:1011–1018.